

1 Report

2

3 Monoclonal antibodies that recognize symbiotic bacteria and hemocytes in the deep-sea

4 vesicomid clam *Phreagena okutanii*

5

6 Kazue Ohishi<sup>1a</sup>, Yoshimitsu Nakamura<sup>1</sup>, Chiho Kusaka<sup>1</sup>, Yukiko Nagai<sup>1, 2</sup>, Masatoshi

7 Nakazawa<sup>3</sup>, Takao Yoshida<sup>1</sup>, Tadashi Maruyama<sup>1b\*</sup>

8

9 <sup>1</sup>Japan Agency for Marine-Earth Science and Technology (JAMSTEC)

10 <sup>2</sup>Graduate School of Environment and Information Sciences, Yokohama National

11 University

12 <sup>3</sup>School of Medicine, Yokohama City University

13

14 Present affiliation

15 <sup>a</sup>Tokyo Polytechnic University, Faculty of Engineering

16 <sup>b</sup>Kitasato University, School of Marine Biosciences

17

18 \*Corresponding author

19 Tadashi Maruyama

20 Kitasato University, School of Marine Biosciences

21 1-15-1 Kitasato, Minami-ku, Sagamihara, Kanagawa 252-0373, Japan

22 E-mail: PEE02660@nifty.ne.jp

23

24 Key words: monoclonal antibody, *Phreagena*, deep sea, symbiotic bacteria, hemocyte

25 Short title: Monoclonal antibodies against deep-sea clam

26

27 **Abstract**

28 Vesicomylid clams, including the genus *Phreagena*, are dominant members of  
29 various deep-sea chemosynthesis-based animal communities. They harbor symbiotic  
30 sulfur-oxidizing bacteria in the epithelial cells of their gill tissue, and the bacteria are  
31 transmitted to the next generations via eggs. We created a monoclonal antibody (mAb)  
32 library against the gill of *P. okutanii* and observed mAb CokG-D1D3 to react to the  
33 symbiotic bacteria and three mAbs (CokG-Y1F7, CokG-J10D2, and CokG-J3G4) to  
34 bind to hemocytes of *P. okutanii*. The signals of mAb CokG-D1D3 were localized in the  
35 epithelial gill cells called bacteriocytes. We also observed a small number of clear  
36 signals of the antibody in the epithelial follicular cells of the ovary. The signals of mAb  
37 CokG-D1D3 almost exactly overlapped those of the anti-*E. coli* GroEL polyclonal  
38 antibody, while, in the gill, the signal areas of the latter seemed to be slightly wider than  
39 those of the former. Among the three mAbs against the hemocytes, mAbs CokG-Y1F7  
40 and CokG-J10D2 reacted to a large fraction of the hemocyte populations, but mAb  
41 CokG-J3G4 reacted to a smaller fraction. mAb CokG-Y1F7 was observed to bind to the  
42 hemocytes distributed widely in the interstitial spaces of various tissues. These

43 monoclonal antibodies are expected to be useful for studying the interactions between  
44 symbiotic bacteria and host cells and the distribution and functions of hemocytes in  
45 deep-sea vesicomid clams.  
46

## 47 **1. Introduction**

48

49 Vesicomylid bivalves are one of the most abundant animals that inhabit deep-sea  
50 chemosynthesis-based ecosystems (Cavanaugh et al., 1981; Felbeck et al., 1981). They  
51 possess large gills with highly packed sulfur-oxidizing bacteria inside the epithelial  
52 cells; however, they have reduced gill ciliary groove, labial palps, and digestive tube  
53 (Boss and Turner, 1980; Cavanaugh, 1983; Fiala-Medioni and Metivier, 1986). The  
54 presence of many symbiotic bacteria in the bacteriocytes in the gill filament has been  
55 confirmed using *in situ* hybridization (Nakamura et al., 2013). The symbiotic bacteria  
56 are transmitted vertically to the offspring via eggs (Cary and Giovannoi, 1993; Ikuta et  
57 al., 2016). In the ovary, symbiotic bacterial cells have been observed in follicle cells and  
58 on egg cells by using transmission electronic microscopy and *in situ* hybridization  
59 (Ikuta et al., 2016). Genome analyses of the symbiotic bacteria in vesicomylid clams  
60 such as *Phreagena okutanii* Kojima and Ohta 1997 and *Calyptogena magnifica* Boss &  
61 Turner, 1980 have shown that the symbionts are composed of a single species:  
62 *Candidatus* (*Ca.*) *Vesicomysocius okutanii* strain HA (Vok) and *Ca.* *Ruthia magnifica*

63 strain Cm (Rma) (Kuwahara et al., 2007; Newton et al., 2007). They have reduced  
64 genomes and lack some genes that are essential for survival; however, they possess  
65 genes for sulfur-oxidizing metabolism, carbon fixation, and synthesis of amino acids  
66 and organic compounds (Kuwahara et al., 2007; Newton et al., 2007). The findings are  
67 consistent with those of a previous stable isotope analysis that showed that the hosts  
68 nutritionally depend on the organic compounds synthesized by the chemosynthetic  
69 symbionts (Le Pennec et al., 1995). Thus, vesicomid clams and their symbiotic  
70 bacteria form an obligatory symbiotic system.

71 The clams are known to possess a unique oxygen transport system. Hemoglobin is  
72 contained in the red hemocyte, which is thought to circulate in the body and transfer  
73 oxygen to tissues (Suzuki et al., 2000). In general, the hemocytes function in  
74 immunological defense against microbial invasion to maintain homeostasis (Bayne,  
75 1983; Hine, 1999; Muroga and Takahashi, 2007; Takahashi and Muroga, 2008;  
76 Donaghy et al., 2009, Tame et al., 2015). The symbiotic bacteria must escape from the  
77 host defense system, including defense by the hemocytes. However, the mechanism  
78 underlying the escape is still unclear.

79 To understand the molecular mechanisms underlying the maintenance of the  
80 symbiosis, tools for marking the protein components are necessary. We constructed a  
81 monoclonal antibody (mAb) library against the gill component of *P. okutanii* and  
82 reported an mAb that reacts against the mucus component secreted from epithelial cells  
83 in the gill (Nakamura et al., 2013: The mAb and hybridoma are available at the  
84 JAMSTEC Marine Biological Sample Database [[http://www.godac.jamstec.go.jp/bio-](http://www.godac.jamstec.go.jp/bio-sample/showDetail.do?menuId=6&sampleId=1090053148)  
85 [sample/showDetail.do?menuId=6&sampleId=1090053148](http://www.godac.jamstec.go.jp/bio-sample/showDetail.do?menuId=6&sampleId=1090053148), IDs, 1090053149 and  
86 1090053150; Accessed on 2017-11-04]). For studying the interaction between the  
87 symbiont and host, markings of the symbionts and hemocytes are mandatory. Here, we  
88 have reported four new mAbs: one mAb that reacts to the symbiotic bacteria and three  
89 mAbs that bind to the hemocytes.

90

## 91 **2. Materials and Methods**

92

93 An mAb library against the gills of *P. okutanii* was generated as described  
94 previously (Nakamura et al., 2013). Briefly, homogenized gills from *P. okutanii*

95 collected during the R/V Natsushima cruise (NT09-06 Leg1: April 24 to May 6, 2009)  
96 by using the ROV *Hyper-Dolphin* (Dive#973) were used as antigens for inoculating  
97 BALB/c mice. The mAb library was constructed using a conventional polyethylene  
98 glycol method (Galfre and Milstein, 1981). Cloning of the hybridoma was performed  
99 three times using the limited dilution method.

100       The binding activity of the mAbs in the supernatant of the hybridoma culture was  
101 examined using indirect immunofluorescence microscopy with 4- $\mu$ m-thin sections of  
102 the gills or ovaries from adult clams or whole bodies of very small immature clams.  
103 These clams were collected using the ROV *Hyper-Dolphin* during cruises of the R/V  
104 Natsushima (NT09-06 Leg1, Dive#973; NT10-08, Dive#1125; NT11-09, Dive#1291  
105 and 1293; NT13-07, Dive#1508 and 1511) and ROV *KAIKO* during the R/V Kairei  
106 cruise (KR12-05, Dive#545) (Inoue 2010, 2011, Oguri 2012, Yoshida 2013). *P. okutanii*  
107 was identified and distinguished from the sibling species *Phreagena soyoae* by partial  
108 sequencing of the cytochrome c oxidase subunit 1 (*COI*) gene (Harada et al., 2009).  
109 The adult tissues and small clams were fixed with 4% paraformaldehyde in seawater for  
110 18 h. The shells of immature clams were removed using decalcifying buffer (Wako Co.,



111 Tokyo), and three very small clams (length of the shell long axis, 16.0, 17.7, and 22.6  
112 mm) were used to prepare the frozen sections. The adult tissues and the three small  
113 clam bodies were frozen-embedded in optimal-cutting-temperature compound in liquid  
114 nitrogen and sliced using a cryomicrotome (Microm HM550; Thermo Fisher Scientific  
115 Inc., Tewksbury, MA). They reacted to the supernatant of the hybridoma culture at 4 °C  
116 for 2 h. After washing with PBS (135 mM NaCl, 2.7 mM KCl, 10 mM Na<sub>2</sub>HPO<sub>4</sub>, and  
117 1.8 mM KH<sub>2</sub>PO<sub>4</sub>, pH 8.0), they were incubated with Alexa Fluor 488-conjugated goat  
118 anti-mouse IgG (Life Technologies Co. Ltd., Wyman, MA) diluted at 1:2000 at 4 °C for  
119 2 h. Simultaneously, the sections reacted with anti-*E. coli* GroEL rabbit polyclonal  
120 antibody (Sigma Aldrich Co. Ltd., St. Louis, MO) diluted at 1:1000, followed by  
121 incubation with Alexa Fluor 647-conjugated anti-rabbit IgG antibodies (Life  
122 Technologies Co. Ltd., Wyman, MA) diluted at 1:2000 at 4 °C for 2 h. The sections  
123 were also stained with 6-diamidino-2-phenylindole dihydrochloride (DAPI; Sigma-  
124 Aldrich Co. Ltd., St. Louis, MO) at a concentration of 10 µg/ml at room temperature for  
125 15 min. For morphological observation, 4-µm-thin sections were obtained from  
126 paraformaldehyde-fixed and paraffin-embedded adult tissues or immature clam bodies.

127 Conventional hematoxylin and eosin (HE) staining was performed, and a microscope  
128 equipped with fluorescence optics (BZ-900; Keyence Co. Ltd., Osaka, Japan) was used  
129 for observation.

130

### 131 **3. Results**

132

#### 133 **3.1 mAb CokG-D1D3 reacted to the symbiotic bacteria in the gills and ovaries of *P.***

134 *okutanii*

135 Newly established mAbs from the mAb library against *P. okutanii* gills are listed  
136 in Table 1. In a transverse section, the gill filament is composed of three parts: the inner  
137 zone containing many symbiont cells and two symbiont-lacking zones, the frontal zone  
138 and the junction area between the inner and the frontal zones (Ohishi et al., 2016; IZ, FZ,  
139 and J in Fig. 1a). Black particles indicating elemental sulfur were observed in the inner  
140 zone of a frozen section (Fig. 1b) (Ohishi et al., 2016). Strong signals for mAb CokG-  
141 D1D3 were detected in only the inner zone (Fig. 1c). No signal was detected in a negative  
142 control using PBS instead of primary antibodies. We concomitantly immunostained the

143 symbionts with the anti-*E. coli* GroEL antibody, which has been used to detect them (Fig.  
144 1d and e; Nakamura et al., 2013; Ohishi et al., 2016). Signals of both the mAb and anti-  
145 *E. coli* GroEL antibody were detected in almost the same area, indicating that this mAb  
146 specifically reacts to the symbiont cells. However, their appearances were different. At  
147 higher magnification, the mAb signals appeared as clear dots in the cytoplasm of the  
148 epithelial cells, called bacteriocytes, of the inner zone (Fig. 2). However, the signals from  
149 the anti-*E. coli* GroEL antibody were not clear but blurred (Fig. 2a, b, and d). In addition,  
150 it is noteworthy that the signals of the anti-*E. coli* GroEL antibody were distributed a little  
151 wider than those of the mAb: red color protruding slightly out of the area containing green  
152 dot (white arrows in Fig. 2d).

153       Because the symbiotic bacteria are vertically transmitted via the female gonad, the  
154 reactivity of mAb CokG-D1D3 to the ovary tissue was examined using frozen sections  
155 from adult female clams. The follicle cells were observed as the epithelium lining the  
156 ovarian cavity (yellow triangles in Fig. 3a), and various maturation stages of the oocytes  
157 were in the cavities (white triangles in Fig. 3a). The dotted signals of the mAb were  
158 clearly observed in the follicle cells, although the number of the dots in a cell (yellow

159 triangles in Fig. 3b and c) was much less than those in the gill (Fig. 2a and d). The  
160 difference in signal appearances between the mAb and anti-*E. coli* GroEL antibody  
161 detected in the gill was less conspicuous in the gonad than in the gill. We could detect no  
162 signal from either mAb or anti-*E. coli* GroEL antibody in the oocytes (white triangles in  
163 Fig. 3b–d). In some immature clams, we observed many ring-like or ellipsoidal structures  
164 in the gonad tissue area at the base of the foot in the HE-stained paraffin-embedded whole  
165 body (black triangles and a dotted ellipse in Fig. 4a), which seemed to be immature  
166 follicle cells in the ovaries. The frozen sections from the three very small clam bodies  
167 were also immunologically stained with mAb CokG-D1D3 or anti-*E. coli* GroEL  
168 antibody. Both signals were observed in the ring-like or ellipsoidal shapes in the gonad  
169 tissue area in the two immature clams (length of the shell long axis, 16.0 mm and 17.7  
170 mm; white arrows and a dotted ellipse in Fig. 4b).

171

### 172 **3.2 mAbs CokG-Y1F7, CokG-J10D2, and CokG-J3G4 reacting to hemocyte-like** 173 **cells in *P. okutanii***

174 The signals of mAbs CokG-Y1F7, CokG-J10D2, and CokG-J3G4 reacted with

175 hemocyte-like cells inside the gill filament (Table 1). Since these cells were  
176 morphologically recognized as hemocytes, the mAbs were thought to react to the  
177 hemocytes. The mAbs CokG-Y1F7 and CokG-J10D2 were bound to a large proportion  
178 of hemocytes in the blood vein-like cavities (Fig. 5a and b), while mAb CokG-J3G4  
179 reacted with a smaller fraction (Fig. 5c). Approximately 80% of the hemocytes in the  
180 images reacted positively with mAbs CokG-Y1F7 and CokG-J10D2 and 40% with mAb  
181 CokG-J3G4. The distribution of the signal-positive cells in the whole bodies of the  
182 immature clams was examined using mAb CokG-Y1F7 because its signal seemed to be  
183 the strongest. The signal-positive cells were found in the cavities of various tissues, such  
184 as the gill and mantle (Fig. 6); however, the signal was also detected on some parts of the  
185 mantle surface facing the shell (white arrow in Fig. 6). In the immature clams, the  
186 hemocyte-like cells were observed in a relatively large cavity at the base of the foot,  
187 which surrounds the intestine (Fig. 7a), although the cavity and hemocyte-like cells were  
188 not well-recognized in the adult clams (data not shown). The mAb CokG-Y1F7 bound to  
189 these cells which seemed to be free-moving cells, indicating that the cells in the cavity  
190 were hemocytes (Fig. 7b). Thus, mAb CokG-Y1F7 recognized the hemocytes in the

191 interstitial space of various tissues.

192

#### 193 **4. Discussion**

194 The dot-like signals of mAb CokG-D1D3 were abundantly found in the  
195 bacteriocytes of the gill, while clear but smaller number of signals were detected in the  
196 follicular cells of the ovary (Figs. 1–3). The dotted signals were found to be restricted to  
197 the symbiosome of the bacteriocyte in the gill filament and follicle cell, where the signal  
198 of the anti-GroEL antibody was also co-localized. Thus, the distribution and number of  
199 signals by mAb CokG-D1D3 were consistent to those of the symbiotic bacteria. These  
200 results indicate that the mAb binds to the symbiotic bacterium of *P. okutanii*, Vok,  
201 although we failed to identify the target antigen by using western blot analysis. A recent  
202 study has shown that approximately 400 cells of the symbiotic bacterium Vok were at the  
203 vegetal pole of the eggs, but they were not found in the sections of other parts of the large  
204 egg cells (Ikuta et al., 2016). This may explain why we could not find the signal for mAb  
205 CokG-D1D3 in the sections of the oocytes. In the basic part of the foot of juvenile clams,  
206 the symbiotic bacteria were located in circularly or elliptically arranged cells (Fig. 4).

207 Although further studies are required, this finding suggests that such small-sized clams  
208 have ovarian follicle cells that already contain the symbionts. The metabolism of the  
209 symbiont in the gill has been suggested to be different from that in the ovary (Ohishi et  
210 al., 2016). This difference is understandable because sulfur oxidation metabolism is  
211 important for maintaining the lives of both partners in the gill; however, its importance is  
212 not clear in the follicle cells where the symbiont must be securely transmitted to the next  
213 generation of the host. Ikuta et al. (2016) raised an important question: How are the  
214 symbionts transferred from the outside surface of the egg to the inside of follicle cells,  
215 oocytes, and gill epithelial cells during development. Although the target antigen is not  
216 known, the symbiont-specific monoclonal antibody, mAb CokG-D1D3, could be useful  
217 for tracing symbiotic bacteria during the development of the clam and/or regeneration  
218 after the accidental or natural death of bacteriocytes. Studying the fate of symbiotic  
219 bacteria during the life cycle of the host clam would be key in understanding how the  
220 symbiosis is maintained.

221 The signals of mAb CokG-D1D3 and anti-*E. coli* GroEL antibody were almost co-  
222 localized in the bacteriocytes in the gill epithelium and ovarian follicle cells (Figs. 2d and

223 3e). However, the signals of the latter formed blurred dots and seemed to expand slightly  
224 more than the former (Figs. 1 and 2). GroEL, a chaperon protein involved in protein  
225 folding, is known to be highly produced in the symbiotic bacterium *Buchnera aphidicola*  
226 (Ishikawa et al., 1984). GroEL in Vok is also highly expressed (Yoshida T, personal  
227 communication). The slightly expanded signal area detected by the anti-*E. coli* GroEL  
228 antibody might be due to the higher production of GroEL in Vok. Recently it has been  
229 shown that some intracellular pathogenic bacterial GroEL possesses multi-functions and  
230 is not always localized in the cytoplasm of the bacteria cells (Garduno et al., 2011). These  
231 questions need to be addressed in the future.

232 We observed that three mAbs (CokG-Y1F7, CokG-J10D2, and CokG-J3G4)  
233 reacted with the hemocytes. Two of them, CokG-Y1F7 and CokG-J10D2, were bound to  
234 a large fraction of the hemocytes, while the third one, CokG-J3G4, reacted to a smaller  
235 fraction. The results may indicate multiple populations in the hemocytes. Alternatively,  
236 the hemocytes may be at different developmental stages or immunological activation  
237 stages. The mAb CokG-Y1F7 bound to the hemocytes in the cavity at the base of the foot  
238 in an immature clam, where premature ovarian follicle cells containing symbiotic bacteria



239 seemed to be localized (Fig. 4). The mAb may be useful for detecting the distribution of  
240 hemocytes in the open blood-vascular system at various developmental stages. Because  
241 hemocytes of bivalves have been shown to play a crucial role in immunological defense  
242 (Bayne, 1983; Hine, 1999; Muroga and Takahashi, 2007; Takahashi and Muroga, 2008;  
243 Donaghy et al., 2009, Tame et al., 2015), it would be interesting to investigate whether  
244 certain types of hemocytes are specifically localized in the symbiont-containing gill tissue  
245 and how the symbiotic bacteria escape from the host defense system. The mAbs are  
246 expected to be useful in addressing these immunological queries by recognizing the  
247 symbiont cells and different types of hemocytes. It is important to establish additional  
248 useful mAbs against various tissue cells or cell components of *P. okutanii* and characterize  
249 them for further studies on symbiosis in deep-sea clams.

250

## 251 **Acknowledgments**

252 The authors thank the chief scientists, captains, and crew of the R/V Natsushima  
253 cruises (NT09-06 Leg1, NT10-08, NT11-09, and NT13-07) and R/V Kairei (KR12-05)  
254 and the operation team of the ROV *Hyper Dolphin* and ROV *KAIKO 7000II* for helping

255 in the collection of the deep-sea biological samples. The authors appreciate Dr. T. Iseto  
256 and Data Management Office of JAMSTEC for their advice about the JAMSTEC  
257 Database. We also thank Editage ([www.editage.jp](http://www.editage.jp)) for English language editing.  
258

259 **Figure Legends**

260

261 Fig. 1. Immunofluorescence micrographs of the monoclonal antibody (mAb) CokG-  
262 D1D3 binding to the gill filament of *Phreagena okutanii*. **a**, HE-stained paraffin-  
263 embedded transverse section of the gill. **b**, Bright-field micrographs of a frozen  
264 transverse section. **c and d**, Fluorescent images with mAb CokG-D1D3 (green) and  
265 anti-*E. coli* GroEL antibody (red). **e**, Triple merged fluorescent images of mAb CokG-  
266 D1D3 (green), anti-*E. coli* GroEL antibody (red), and DAPI (blue). Scale bars indicate  
267 50  $\mu\text{m}$  (**a**) and 20  $\mu\text{m}$  (**b–d**). IZ, inner zone; FZ, frontal zone; J, junction area between  
268 IZ and FZ.

269

270 Fig. 2. Higher-magnification immunofluorescence micrograph of the monoclonal  
271 antibody (mAb) CokG-D1D3 binding to the gill filament of *Phreagena okutanii*. **a–c**,  
272 Fluorescent images with mAb CokG-D1D3 (**a**, green), anti-*E. coli* GroEL antibody (**b**,  
273 red), and DAPI (**c**, blue) of the same frozen transverse section of a gill filament. **d**,  
274 Triple merged fluorescent images of mAb CokG-D1D3 (green), anti-*E. coli* GroEL

275 antibody (red), and DAPI (blue). White arrows indicate the wider stained area with anti-  
276 *E. coli* GroEL antibody than that with mAb CokG-D1D3. Scale bar, 40  $\mu\text{m}$ .

277

278 Fig. 3. Immunofluorescence micrographs of the monoclonal antibody (mAb) CokG-  
279 D1D3 bound to the ovary of *Phreagena okutanii*. **a**, HE-stained thin section of the  
280 paraffin-embedded ovary. **b**, Bright-field micrographs of a frozen transverse section. **c**  
281 and **d**, Fluorescent images with mAb CokG-D1D3 (green) and anti-*E. coli* GroEL  
282 antibody (red). **e**, Triple merged fluorescent images of mAb CokG-D1D3 (green), anti-  
283 *E. coli* GroEL antibody (red), and DAPI (blue). Scale bars indicate 100  $\mu\text{m}$  (**a**) and 40  
284  $\mu\text{m}$  (**b–d**). Yellow triangles: follicular cells, white triangles: oocytes.

285

286 Fig. 4. Immunofluorescence micrographs of the monoclonal antibody (mAb) CokG-  
287 D1D3 bound to an immature *Phreagena okutanii*. **a**, HE-stained cross-section of  
288 paraffin-embedded whole immature clams. **b**, Triple merged fluorescent images of mAb  
289 CokG-D1D3 (green), anti-*E. coli* GroEL antibody (red), and DAPI (blue) in a frozen  
290 section of the whole immature clams. Scale bars indicate 500  $\mu\text{m}$  (**a**) and 40  $\mu\text{m}$  (**b**).

291 Black triangles and white triangles indicate immature ovary-like ellipsoidal structures. A  
292 structure was surrounded by black or white dotted ellipses.

293

294 Fig. 5. Immunofluorescence micrographs of the monoclonal antibodies (mAbs) reacting  
295 to hemocytes inside the gill filaments of *Phreagena okutanii*. **a**, Merged fluorescent  
296 images of mAb CokG-Y1F7 (green) and DAPI (blue). **b**, Merged images of mAb  
297 CokG-J10D2 (green), DAPI (blue), and bright-field micrographs. **c**, Merged images of  
298 mAb CokG-J3G4 (green), DAPI (blue), and bright-field micrographs. Scale bars  
299 indicate 40  $\mu\text{m}$  (**a**, **b**, and **c**). Haze reduction function (Keyence fluorescence  
300 microscope) was used for (**a**).

301

302 Fig. 6. Immunofluorescence micrographs of the monoclonal antibody (mAb) CokG-  
303 Y1F7 in frozen whole sections from immature *Phreagena okutanii*. **a**, Bright-field  
304 micrographs of the frozen cross-section. **b**, Fluorescent image of mAb CokG-Y1F7  
305 (green). **c**, Merged fluorescent images of CokG-Y1F7 (green) and DAPI (blue) in the  
306 mantle. White arrow indicates a part of the mantle binding to mAb CokG-Y1F7. Scale

307 bars indicate 50  $\mu\text{m}$  (**a**, **b**) and 30  $\mu\text{m}$  (**c**). Haze reduction function (Keyence

308 fluorescence microscope) was used for (**c**).

309

310 Fig. 7. Immunofluorescence micrographs of the monoclonal antibody (mAb) CokG-

311 Y1F7 bound to hemocyte-like cells in a cavity surrounding the intestine of immature

312 *Phreagena okutanii*. Paraffin-embedded section from an immature clam with a body

313 length of 20 mm was used. **a**, Bright-field micrographs of the section. **b**, Fluorescent

314 image of mAb CokG-Y1F7 (green). Scale bars indicate 30  $\mu\text{m}$ .

315

316

317 **References**

318

319 Bayne, C. J. (1983), *Molluscan Immunology*, Academic Press, London.

320 Boss, K. J., and R. D. Turner (1980), The giant white clam from the Galapagos rift,

321 *Calyptogena magnifica*, sp. n. *Malacologia*, 20, 161–194.

322 Cary, S. C., and S. J. Giovannoni (1993), Transovarial inheritance of endosymbiotic

323 bacteria in clams inhabiting deep-sea hydrothermal vents and cold seeps, *Proc.*

324 *Natl. Acad. Sci. USA*, 90, 5695–5699.

325 Cavanaugh, C. M., S. L. Gardiner, M. L. Jones, H. W. Jannasch, and J. B. Waterbury

326 (1981), Prokaryotic cells in the hydrothermal vent tube worm *Riftia pachyptila*

327 Jones: possible chemoautotrophic symbionts, *Science*, 213, 340–342.

328 Cavanaugh, C. M. (1983), Symbiotic chemoautotrophic bacteria in marine invertebrates

329 from sulphide-rich habitats, *Nature*, 302, 58–61.

330 Donaghy, L., C. Lambert, K.-S. Choi, and P. Soudant (2009), Hemocytes of the carpet

331 shell clam (*Ruditapes decussatus*) and the Manila clam (*Ruditapes*

332 *philippinarum*): current knowledge and future prospects, *Aquaculture*, 297,

333 10–24.

334 Felbeck, H., J. J. Childress, and G. N. Somero (1981), Calvin-Benson cycle and  
335 sulphide oxidation enzymes in animals from sulphide-rich habitats, *Nature*,  
336 293, 291–293.

337 Fiala-Medioni, A., and C. Metivier (1986), Ultrastructure of the gill of the hydrothermal  
338 vent bivalve *Calyptogena magnifica*, with a discussion of its nutrition, *Mar.*  
339 *Biol.*, 90, 215–222.

340 Galfre, G. and C. Milstein (1981), Preparation of monoclonal antibodies: strategies and  
341 procedures, *Methods in Enzymology*, 73, 3–46.

342 Garduno, R. A., A. Chong, G. K. Nasrallah, and D. S. Allan (2011), The *Legionella*  
343 *pneumophila* chaperonin – An unusual multifunctional protein in unusual  
344 locations, *Front. Microbiol.* doi: 10.3389/fmicb.2011.00122.

345 Harada, M., T. Yoshida, H. Kuwahara, S. Shimamura, Y. Takaki, C. Kato, T. Miwa, H.  
346 Miyake, and T. Maruyama (2009), Expression of genes for sulfur oxidation in  
347 the intercellular chemoautotrophic symbiont of the deep-sea bivalve  
348 *Calyptogena okutanii*, *Extremophiles*, 13, 895–903.

349 Hine, P. M. (1999), The inter-relationships of bivalve haemocytes, *Fish Shellfish*  
350 *Immunol.*, 9, 367–385.

351 Ikuta T, K. Igawa, A. Tame, T. Kuroiwa, H. Kuroiwa, Y. Aoki, Y. Takai, Y. Nagai, G.  
352 Ozawa, M. Yamamoto, R. Deguchi, K. Fujikura, T. Maruyama, and T.  
353 Yoshida (2016), Surfing the vegetal pole in a small population: extracellular



354 vertical transmission of an ‘intracellular’ deep-sea clam symbiont, *R. Soc.*  
355 *Open Sci.*, 3:160130. doi:10.1098/rsos.160130.

356 Inoue, K. (2010), NATSUSHIMA Cruise report NT10-08, *NATSUSHIMA Cruise report*,  
357 [http://www.godac.jamstec.go.jp/catalog/data/doc\\_catalog/media/NT10-](http://www.godac.jamstec.go.jp/catalog/data/doc_catalog/media/NT10-08_all.pdf)  
358 [08\\_all.pdf](http://www.godac.jamstec.go.jp/catalog/data/doc_catalog/media/NT10-08_all.pdf).

359 Inoue, K. (2011), RV Natsushima Cruise Report NT11-09, NATSUSHIMA Cruise  
360 report,  
361 [http://www.godac.jamstec.go.jp/catalog/data/doc\\_catalog/media/NT11-](http://www.godac.jamstec.go.jp/catalog/data/doc_catalog/media/NT11-09_all.pdf)  
362 [09\\_all.pdf](http://www.godac.jamstec.go.jp/catalog/data/doc_catalog/media/NT11-09_all.pdf).

363 Ishikawa, H. (1984), Alteration with age of symbiosis of gene expression in aphid  
364 symbionts, *Biosystems*, 17, 127–134.

365 Kuwahara, H., T. Yoshida, Y. Takaki, S. Shimamura, S. Nishi, M. Harada, M., Matsuyama,  
366 K., Takishita, M., Kawato, K., Uematsu, K., Fujiwara, T., Sato, C., Kato, M.  
367 Kitagawa, I. Kato, and T. Maruyama (2007), Reduced genome of the thioautotrophic  
368 intracellular symbiont in a deep-sea clam, *Calymptogena okutanii*, *Curr. Biol.*, 17,  
369 881–886.

370 Le Pennec M, P. G. Beninger, and A. Herry (1995), Feeding and digestive adaptations of  
371 bivalve molluscs to sulphide-rich habitats, *Comp. Biochem. Physiol. A*  
372 *Physiol.*,*III*, 183–189.

373 Muroga K, and K. Takahashi (2007), Review on the studies of humoral defense factors  
374 in bivalve mollusks, *Fish Pathol.*, *42*, 1–17. (in Japanese with English  
375 abstract)

376 Nakamura, Y, M. Konishi, K. Ohishi, C. Kusaka, A. Tame, Y. Hatada, K. Fujikura, M.  
377 Nakazawa, M. Fujishima, T. Yoshida, and T. Maruyama (2013), Mucus  
378 glycoproteins selectively secreted from bacteriocytes in gill filaments of the  
379 deep-sea clam *Calyptogena okutanii*, *Open J. Mar. Sci.*, *3*, 167–174.

380 Newton, I. L., T. Woyke, T. A. Auchtung, G. F. Dilly, R. J. Dutton, M. C. Fisher, K. M.  
381 Fontanez, E. Lau, F. J. Stewart, P. M. Richardson, K. W. Barry, E. Saunders,  
382 J. C. Detter, D. Wu, J. A. Eisen, and C. M. Cavanaugh (2007), The  
383 *Calyptogena magnifica* chemoautotrophic symbiont genome, *Science*, *315*,  
384 998–1000.

385 Oguri K. (2012), ROV KAIKO7000II & R/V KAIREI, KR12-05.

386 [http://www.godac.jamstec.go.jp/catalog/data/doc\\_catalog/media/KR12-](http://www.godac.jamstec.go.jp/catalog/data/doc_catalog/media/KR12-)  
387 [05\\_all.pdf](#)

388 Ohishi, K., M. Yamamoto, A. Tame, C. Kusaka, Y. Nagai, M. Sugimura, K. Inoue, K.  
389 Uematsu, T. Yoshida, T. Ikuta, T. Toyofuku, and T. Maruyama (2016), Long-  
390 term cultivation of the deep-sea clam *Calyptogena okutanii*: changes in the  
391 abundance of chemoautotrophic symbiont, elemental sulfur, and mucus. *Biol.*  
392 *Bull.*, 230, 257–267.

393 Suzuki T, H. Kawamichi, R. Ohtsuki, M. Iwai, and K. Fujikura (2000), Isolation and  
394 cDNA-derived amino acid sequences of hemoglobin and myoglobin from the  
395 deep-sea clam *Calyptogena kaikoi*, *Biochim. Biophys. Acta.*, 1478, 152–158.

396 Takahashi, K. and K. Muroga (2008), Review: Cellular defense mechanisms in  
397 bivalves. *Fish Pathol.*, 43, 1–17. (in Japanese with English abstract)

398 Tame, A., T. Yoshida, K. Ohishi, and T. Maruyama (2015) Phagocytic activities of  
399 hemocytes from the deep-sea symbiotic mussels *Bathymodiolus japonicus*, *B.*  
400 *platifrons*, and *B. septemedierum*, *Fish Shellfish Immunol.*, 45, 146–156.

401 Yoshida, T. (2013), RV Natsushima Cruise Report NT13-07, NATSUSHIMA Cruise

402 report,

403 [http://www.godac.jamstec.go.jp/catalog/data/doc\\_catalog/media/NT13-](http://www.godac.jamstec.go.jp/catalog/data/doc_catalog/media/NT13-)

404 [07\\_all.pdf](#).

405

406 Table 1. List of the mAbs to *Phreagena okutanii*

407

mAb ID No.	Targets of mAb	JAMSTEC Database ID*	
		Antibody (supernatant)	Hybridoma cell
CokG-D1D3	Symbiotic bacteria	1090053151	1090053152
CokG-Y1F7	Hemocyte	1090053153	1090053154
CokG-J10D2	Hemocyte	1090053155	1090053156
CokG-J3G4	Hemocyte	1090053157	1090053158

408

409 \*, mAb and hybridoma cell line are available. Please see Japan Agency for

410 Marine-Earth Science and Technology (JAMSTEC), Marine Biological Sample

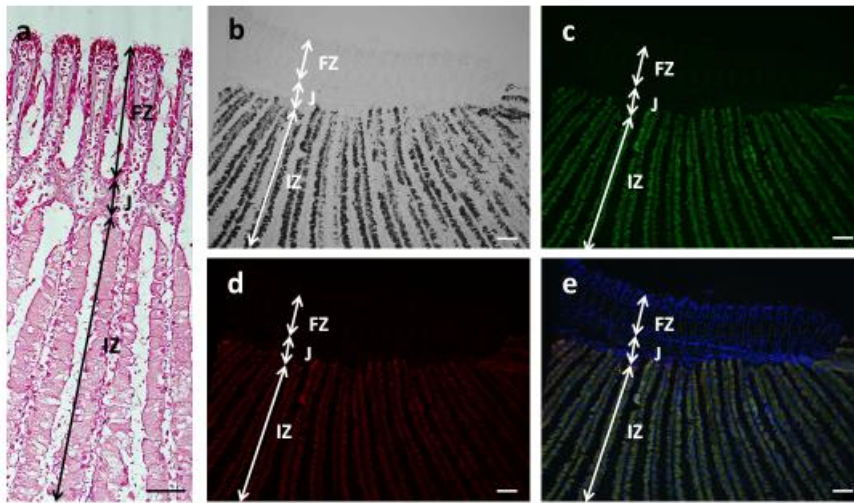
411 Database

412 (<http://www.godac.jamstec.go.jp/bio-sample/showDetail.do?menuId=6&sampleId=109>

413 [0053148](http://www.godac.jamstec.go.jp/bio-sample/showDetail.do?menuId=6&sampleId=1090053148), Accessed on 2017-11-04)

414

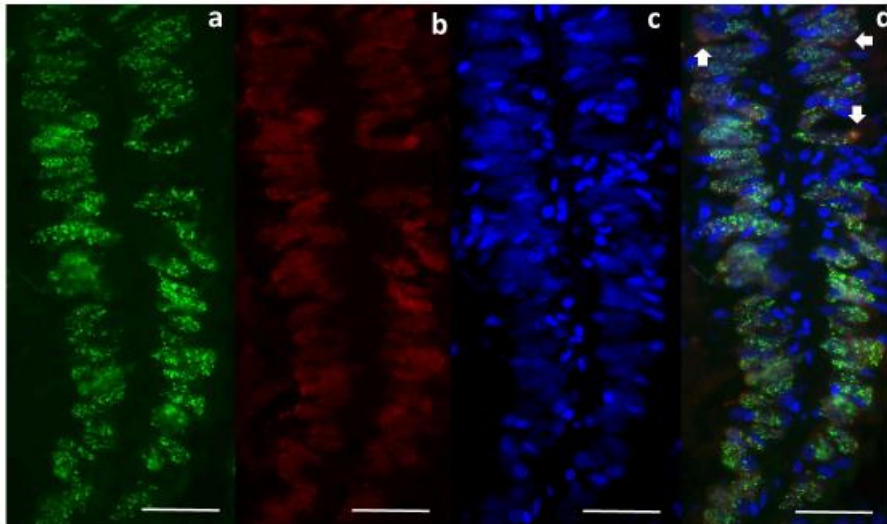
Fig. 1



415

416

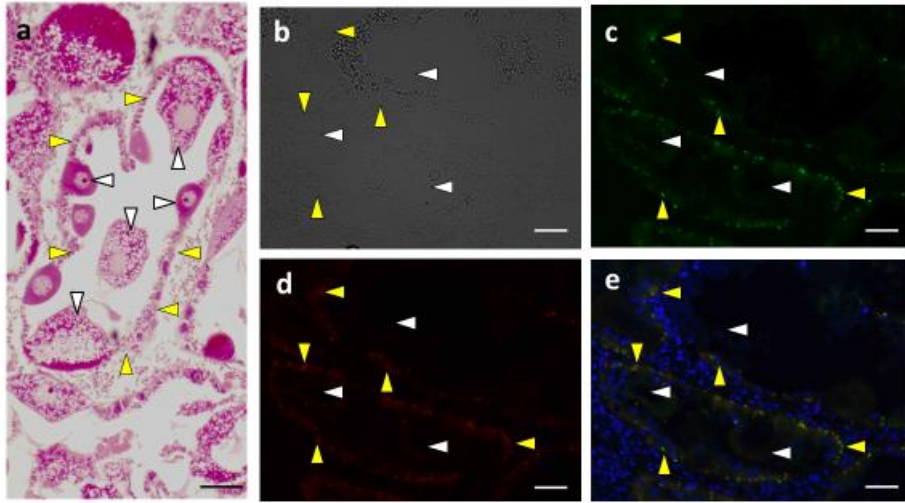
Fig. 2



417

418

Fig. 3

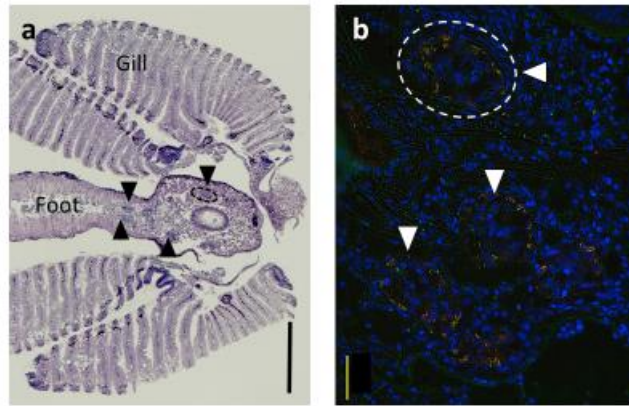


419

420



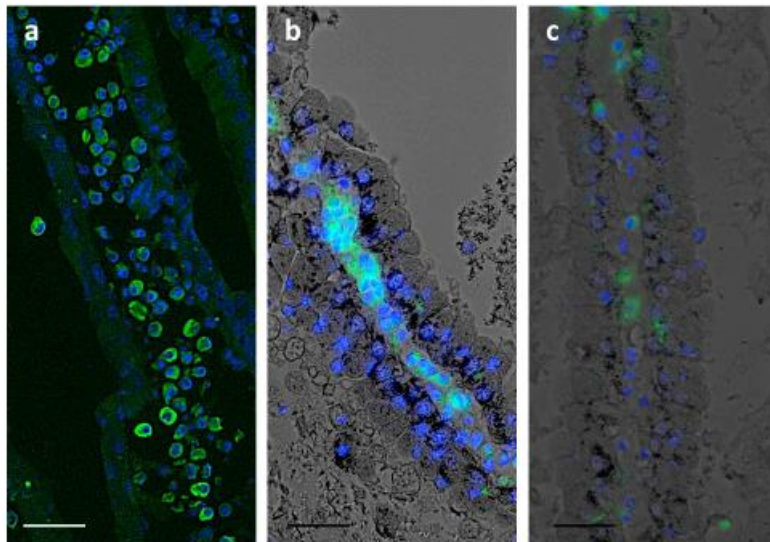
Fig. 4



421

422

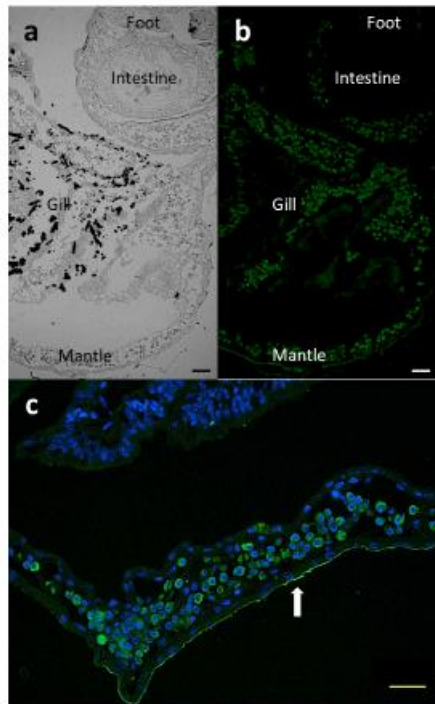
Fig.5



423

424

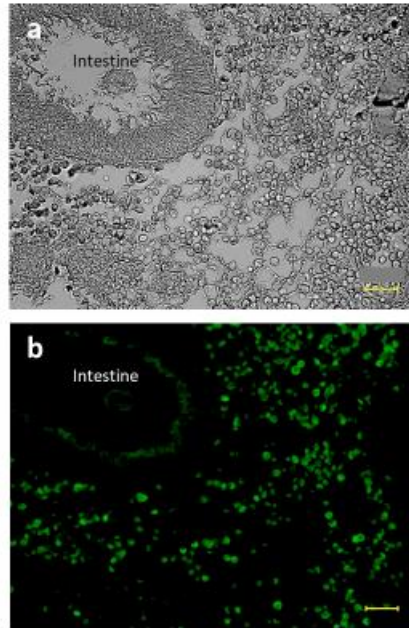
Fig. 6



425

426

Fig.7



427